報 文
화학공학 제 11 권, 제 5 호
J. KIChE. Vol. 11, No. 5
Oct. 1973

An Analysis of Cooling-Type Continuous Crystallizers

*Roy D. Sarcona · *Chang Dae Han

(접수 73. 8. 10)

Abstract

A mathematical model is derived describing the steady state operation of a continuous cooling-type crystallizer. The system considered for testing the model is magnesium sulfate heptahydrate-water. Nucleation and growth rate expressions for the system are derived from experimental data obtained from the literature. A computer program was developed so as to facilitate solution of the non-linear system equations. The model was tested with various sets of hypothetical input data so as to determine crystallizer and heat exchanger design parameters given the data describing the desired steady state operation, and to determine the effect of changes in steady state operating conditions on crystallizer output (particle size distribution and yield). The techniques developed in this study provide a means to the solution of pertinent engineering problems associated with this type of crystallization process.

1. Introduction

The use of crystallization as a unit operation is widespread throughout the chemical industry. It is a prime method of purification and separation in many chemical processes. However, until recent years the theory associated with this process lacked the mathematical description normally required for design calculations or for accurate predictions of the results arising from fluctuations in steady operating conditions. This also prevented the direct application of modern process control techniques.

The development of particle conservation equations and methods measuring crystal growth and nucleation rates have facilitated the derivation of a mathematical description of the crystallization process(1, 2.) Numeros authors have investigated nucleation and growth rate kinetics for both specific and general crystallization systems(3, 4). The dynamic aspects of isothermal crystallizer operation have also been explored to a wide degree (5, 6, 7). Steady state analyses of isothermal well-mixed crystallizers have also been performed with an emphasis being placed on such areas as staging and classification of fines(8, 9, 10).

There still remains the need for a model that can be readily applied to the practical engineering problems of design and operational investigation of existing installations. The primary objective of the present study was to develop and test such a model for a contiuous forced circulation cooling-type crystallizer using magnesium sulfate heptahydrate-water as the crystallization medium.

The results obtained from testing this model with various sets of steady state operating conditions are specific for the system under investigation. However, the techniques illustrated in this study can be extended to other crystallation systems thereby providing a completely general method for both design and control.

2. Mathematical Development

The system under consideration is shown schematically in Figure 1. The fresh feed stream is unsturated

*Department of Chemical Engineering Polytechnic Institute of Brooklyn Brooklyn, N. Y. 11201

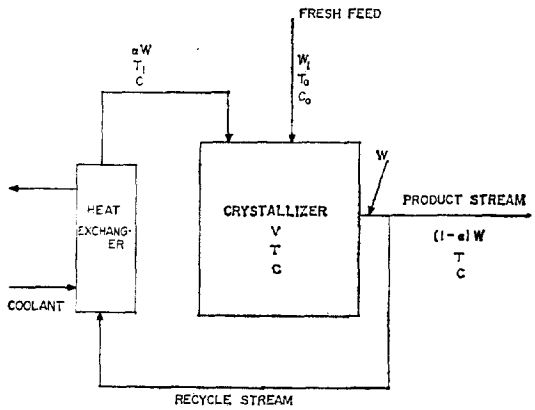

Fig. 1 Schematic diagram of the crystallization system

containing solute at a concentration of C_0 lbm./ft³. and is at a temperature T_0(°F). The crystallizer is well mixed at a uniform temperature T(°F) and concentration C (lbm./ft³.) which is in excess of the saturation concentration. The recycle stream passing through the heat exchanger is cooled to temperature T_1 (°F). The fresh feed is delivered at a constant flow rate W_1 ft³./hr. The product stream is whitdrawn at a rate of $(1-\alpha)W$ ft³./hr., where α is the recycle ratio and W is the total volumetric flow rate from the crystallizer.

The flow of the recycle stream through the heat exchanger is assumed not to affect the particle size distribution or the solute concentration due to restrictions on temperature drop and tubular velocity.

The following assumptions are made in order to facilitate the development of the appropriate conservations: (1) the volume of a crystal can be written as Kr^3 where r is a linear dimension and K is the appropriate shape factor, (2) the crystal density ρ (lbm./ft³.) is constant, (3)the growth rate of the crystal is independent of the size and can be expressed as a function of concentration and temperature:

$$\frac{dr}{dt}=G(C, T) \tag{1}$$

and (4) the crystallizer volume occupied by the magma (V) is assumed constant.

The particle size distribution in the crystallizer f (r, t), is defined as the number of crystals per unit volume having a radius between r and $r+dr$ at time t.

The appropriate conservation equations can now be written. The particle balance equation is as follows:

$$V\frac{\partial f}{\partial t}+GV\frac{\partial f}{\partial r}=\varepsilon BV\delta(r-r_0)-(1-\alpha)Wf \quad r>0 \tag{2}$$

in which ε is the volume fraction of solution, $1-\alpha=\int_0^\infty Kr^3f(r,t)dr$ is the volume fraction of solids, and B is the nucleation rate (number particles/ ft³./ hr.). The term $\delta(r-r_0)$ implies that all new crystals are nucleated at size r_0. In addition, it should be noted that $f(r,t)=0$ for $r\leq 0$.

The conservation of solute is governed by the relation:

$$V\frac{d[\varepsilon C+(1-\varepsilon)\rho]}{dt}=W_1C_0+\alpha W[\varepsilon C+(1-\varepsilon)\rho]-W[\varepsilon C+(1-\varepsilon)\rho] \tag{3}$$

The heat balance equation is given by

$$V\rho_m Cp_m\frac{dT}{dt}=\rho_f C_{pf}W_1T_0-(1-\alpha)WC_{p_s}\rho_d T+W(1-\alpha)(1-\varepsilon)\rho\Delta H_C-Q \tag{4}$$

The particle balance equation (2) is now multiplied by Kr^3 and integrated over r, giving rise to

$$V\frac{d(1-\varepsilon)}{dt}=GV\sigma+VB\varepsilon Kr_0^3-(1-\alpha)W(1-\varepsilon) \tag{5}$$

where

$$\sigma=3K\int_0^\infty r^2fdr \tag{6}$$

Combining Equation (5) with the solute conservation relation (Equation (3)) yields the following:

$$V\varepsilon\frac{dC}{dt}=W_1C_0-(1-\alpha)WC-(\rho-C)(GV\sigma+VB\varepsilon Kr_0^3) \tag{7}$$

Thus, the crystallization system is completely defined by the set of equations (2), (4), and (7).

Equation (2) is a partial differential equation in terms of $f(r,t)$. This may be transformed into a set of ordinary differential equations by multiplying successive powers of r^n $(n=0, 1, 2, 3)$ and integrating the resulting equations from $r=0$ to $r=\infty$. The final exp-

pressions may be written as follows (6):

$$V\frac{d\mu_0}{dt}=VB\varepsilon-(1-\varepsilon)W\mu_0 \tag{8}$$

$$V\frac{d\mu_1}{dt}=GV\mu_0+VB\varepsilon r_0-(1-\alpha)W\mu_1 \tag{9}$$

$$V\frac{d\mu_2}{dt}=2GV\mu_1+VB\varepsilon r_0^2-(1-\alpha)\ W\mu_2 \tag{10}$$

$$V\frac{d\mu_3}{dt}=3GV\mu_2+VB\varepsilon r_0^3-(1-\alpha)\ W\mu_3 \tag{11}$$

If we employ the following assumptions to further simplify the system equations:

1) $r_0=0$: This implies that the initial size of the nucleus is assumed to be negligible as compared to the average particle size;
2) $W_1=(1-\alpha)W$: This arises from the fact that the working volume remains constant;
3) $C_p=1/\rho$: Where C_p=Btu/lbm. °F, ρ=grm./cc. This is a frequently employed assumption when specific data is not available. Thus,

$$\rho C_p=62.43\ \text{Btu/ft}^3.$$

for all process streams;
4) A reference temperature of 32°F is assumed in all sensible heat balance computations;
5) $\varepsilon=1-K\mu_3$
6) $\sigma=3K\int_0^\infty r^2 f dr=3K\mu_2$

We obtain the following closed set of dynamic equations which govern the crystallization process:

$$V\frac{d\mu_0}{dt}=VB(1-K\mu_3)-W_1\mu_0 \tag{12}$$

$$V\frac{d\mu_1}{dt}=GV\mu_0-W_1\mu_1 \tag{13}$$

$$V\frac{d\mu_2}{dt}=2GV\mu_2-W_1\mu_2 \tag{14}$$

$$V\frac{d\mu_3}{dt}=3GV\mu_2-W_1\mu_3 \tag{15}$$

$$V(1-K\mu_3)\ \frac{dC}{dt}=W_1(C_0-C)-3K\mu_2VG\ (\rho-C) \tag{16}$$

$$62.43V\ \frac{dT}{dt}=62.43W_1(T_0-T)+W_1K\mu_3\rho\Delta H_C-Q \tag{17}$$

At steady state all parameters cease to be time variant. Therefore, the steady state relationships for this system are as follows:

$$0=B-BK\mu_3-\frac{W_1\mu_0}{V} \tag{18}$$

$$0=G\mu_0-\frac{W_1\mu_1}{V} \tag{19}$$

$$0=2G\mu_1-\frac{W_1\mu_2}{V} \tag{20}$$

$$0=3G\mu_2-\frac{W_1\mu_3}{V} \tag{21}$$

$$0=\frac{W_1(C_0-C)}{V}-3K\mu_2VG(\rho-C) \tag{22}$$

$$0=62.43W_1\ (T_0-T)+W_1\rho K\mu_3\Delta H_C-Q \tag{23}$$

3. The Crystallizaton System

In order to solve the system equations for a specified set of operating conditions a crystallization system had to be selected for which the functional relations for growth, nucleation and solubility are well defined over the working temperature and concentration range.

The magnesium sulfate heptahydrate-water system was selected due to the availability of extensive. nucleation and growth rate data in the literature(11). The solubility data for this is as follows (12):

Gm. $MgSO_4\cdot7H_2O$/100 gm. Soln.	T(°C)
48.4	10
53.6	20
59.4	30
64.2	40

$MgSO_4\cdot7H_2O(X)$	T(°K)
.064	283
.078	293
.097	303
.116	313

A plot of In X vs. $1/T$ ($1/°K$) is given in Fig. 2, yielding a straight line having the equation

$$\text{In}\ X=\frac{-1752}{T}+3,442 \tag{24}$$

The growth rate expression was derived from data

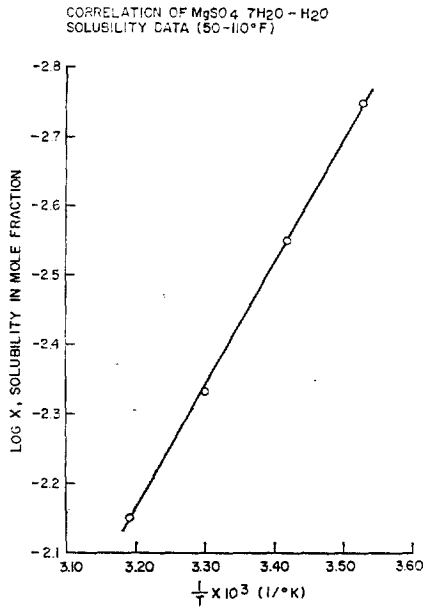

Fig. 2 Correlation of $MgSO_4 \cdot 7H_2O$ solubility data (50~110°F).

obtained by Bransom and Brown (11) on crystallization of $MgSO_4 \cdot 7H_2O$ in a continuous flow stirred-tank me -dium. Their results indicated a non-zero growth rate at zero percent supersaturation. This is clearly evident from the following data (11):

Temperature (°C)	Growth Rate (Ff./Min.)
18.0	$3.50S_1-1.510$
24.3	$5.25S_1-1.880$
35.0	$10.59S_1-0.470$

where S_1 is the percent supersaturation defined as

$$S_1 = 10^2 \left[\frac{C-C_S}{C}\right] \tag{25}$$

in which C_S is the saturated concentration, which is related to X by

$$C_S = \frac{81.0}{0.927 + \dfrac{0.073}{X}} \tag{26}$$

The data indicated the following general form of the equation for growth rate as a function of temperature and concentration:

$$G = K_1(T)S_1 - K_2 \tag{27}$$

where K_1 and K_2 are constants, characteristic of a crystallization system.

The coefficient $K_1(T)$ was found to follow the Arrhenius equation. A plot of In K_1 versus $1/T$ (1/°K) yielded the following relation (Fig. 3):

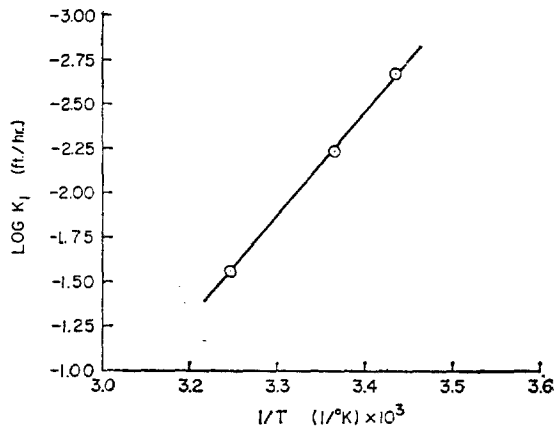

Fig. 3 Correlation of growth rate for $MgSO_4 \cdot 7H_2O$ in H_2O.

$$K_1(T) = 3.84 \times 10^7 \ \mathrm{EXP}\left[\frac{-5862}{T}\right] \tag{28}$$

The second constant, K_2, did not exhibit any general known function of temperature. However, for small fluctuations in temperature about existing data points the value of K_2 can be assumed to be constant. Thus, the expression for growth rate as a function of temperature and concentration is therefore:

$$G = 3.84 \times 10^7 \ \mathrm{EXP}\left[\frac{-5862}{T}\right]\left[\frac{C-C_S}{C_S}\right] - 0.19685 \times 10^{-3} K_2 \tag{29}$$

where K_2 has the following values:

K_2	T(°C)
1.51	18.0
1.88	24.3
0.47	35.0

The nucleation rate expression for $MgSO_4 \cdot 7H_2O$ in H_2O was obtained from the literature in the same manner as the growth rate expression (11):

$$B = 32.0 \times 10^9 \ \mathrm{EXP}\left[\frac{-5090}{T}\right](C-C_S)^4 \tag{30}$$

The remaining required data for the crystallization system was obtained from standard sources (12) and is summarized as follows:

Crystal density = 105.0 lbm./ft³.
Heat of crystallization = 23.2 Btu/lbm.
Shape factor = 0.47

4. Testing the Model

The selected crystallization system was analyzed through the use of the model so as to illustrate its application in the areas of design and process control. The technique employed in each case consisted of assigning hypothetical values to the desired operating variables. This served as input data for the system model. The output was comprised of the calculated values for the remaining parameters in addition to all other associated process data (i. e. particle size distribution, yield, recycle ratio). Hence, a complete description of the steady state crystallization process for the selected system and equipment was obtained for each set of input data.

The correlation of various sets of input and output data provided functional relationships directly applicable to design and contol of the operation. The selection of C_0, C, T_0, T, T_1 and W_1 as input data (i. e. assigned values) gave rise to simplified expressions for the recycle ratio, yield and heat exchanger design. The derivation of these relationships is presented as follows:

4.1 Recycle Ratio

The rate of heat removal for the system is equivalent to the sensible heat change of the recycle stream passing through the heat exchanger. This relation can be expressed in the following manner:

$$Q = \alpha W C_{pr}\rho_r (T - T_1) \tag{31}$$

Equation (31) is now modified via the following substitutions:

$$W = \frac{W_1}{(1-\alpha)} \tag{32}$$

$$C_{pr}\rho_r = 62.43 \tag{33}$$

Thus, combining equations (31), (32) and (33) yields an alternative expression for Q:

$$Q = \frac{62.43\,\alpha W_1 (T - T_1)}{(1-\alpha)} \tag{34}$$

Rearrangement of equation (34) gives rise to the desired relation for the recycle ratio:

$$\alpha = \frac{Q}{Q + 62.43\,W_1 (T - T_1)} \tag{35}$$

Thus, α can be calculated directly from the input and output data associated the system model.

4.2 Yield

The crystallizer yield is defined as the fraction of the solute in the fresh feed appearing as crystal in the product stream. The application of this definition to the system under consideration gives rise to the following relation.

$$Y = \frac{W\rho(1-\varepsilon)(1-\alpha)}{W_1 C_0} \tag{36}$$

Equation (36) can be expressed as follows:

$$Y = \frac{K\mu_3\rho}{C_0} \tag{37}$$

Thus, the yield for this system can be calculated directly from the 3rd moment of the particle size distribution.

4.3 Heat Exchanger Design

The following conditions must be imposed on the heat exchanger operation so as to substantiate the assumption of no change in particle size distribution or solute concentration in the unit (13, 14): (a) the temperature drop of the recycle stream is not greater than 2°F, (b) the maximum logarithmic mean temperature difference for the heat exchanger is 10°F, (c) the heat exchanger is single pass, and (d) the tube velocity is restricted to 5 to 7 ft./sec.

These restraints coupled with the knowledge of the overall heat transfer coefficient and the temperature of the available coolant (assumed to be water) lead to a direct method for determining the heat exchanger design. The total volumetric flow rate of the recycle stream can be expressed as a function of velocity and cross-sectional area:

$$\alpha W = \nu A_i \tag{38}$$

where

$$A_i = \frac{n\pi (D_i)^2}{4} \tag{39}$$

Combining equations (38) and (39) yields the design

relation for the number of exchanger tubes as a function of the inside diameter (given the maximum tubular velocity):

$$n = \left[\frac{4\alpha W_1}{(1-\alpha)\pi\nu_{max}}\right]\frac{1}{(D_i)^2} \tag{40}$$

A similar relation for tube length can be obtained via combination of equation(40) with the overall heat transfer rate equation:

$$L = \left[\frac{A_0}{n\pi}\right]\frac{1}{D_0} \tag{41}$$

where

$$A_0 = \frac{Q}{U_0 \Delta T_{lm}} \tag{42}$$

Thus, for each type of standard heat exchanger tubing (known D_i and D_o), equations (40), (41), and (42) can be employed to generate the required design information. By testing a wide range of tube sizes and comparing the resultant dimensions, a practical heat exchanger design can be obtained.

5. Results and Discussion

The information obtained from each of the case studies can be grouped into the two general categories, namely design and on-line operation. It should be noted that the functional relationships derived from these studies are only applicable to the system being investigated and in most cases cannot be further extended to other crystallization systems. The results presented below are obtained by numerically solving a set of system equations (18)—(23), with the aid of equations (24)—(30).

5.1 Application to Process Design

Figure 4 illustrates the variation of crystallizer volume with the fresh feed flow rate. In essence, it is the relationship between equipment size and throughput. The yield and particle size distribution were invariant over the range of flow rates tested in the model. Analysis of the system equations indicates that in order to maintain a constant process output (i.e. yield, particle size distribution) under conditions of varying production rates, the residence time(expressed as V/W_1) must also be constant.

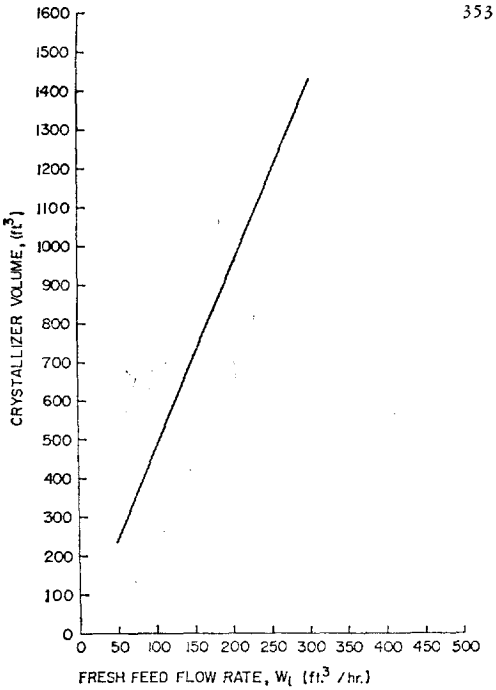

Fig. 4 Crystallizer volume vs. flow rate at the following conditions:
T_0=100°F, T=65°F, C_0=43.48 lbm./ft.³ and C=43.38 lbm./ft³.

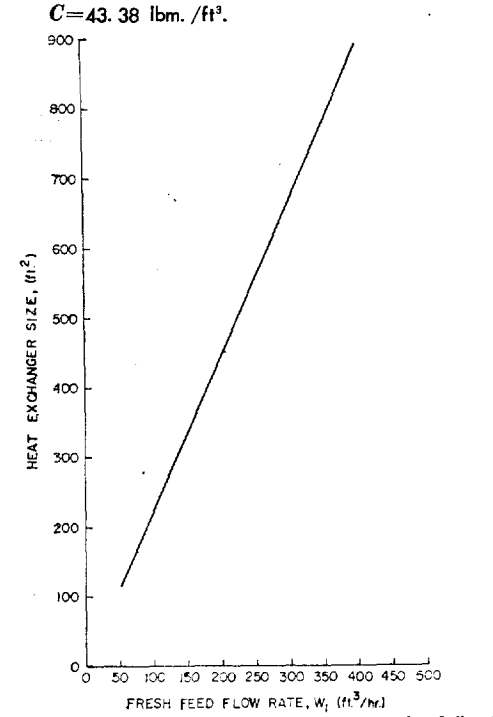

Fig. 5 Heat exchanger size vs. flow rate at the following conditions:
T_0=100°F, T=65°F, C_0=43.48 lbm./ft³., C=43.38 lbm./ft³., U=100 Btu/hr. ft². °F, ΔT_{lm}=10°F.

The linear relationship presented in Figure 5 illustraies the variation of heat exchanger size with throughput rate. The data was obtained with all other process variables maintained at constant values. It should be noted that the total heat duty for the system exhibits a similar variation with production rate.

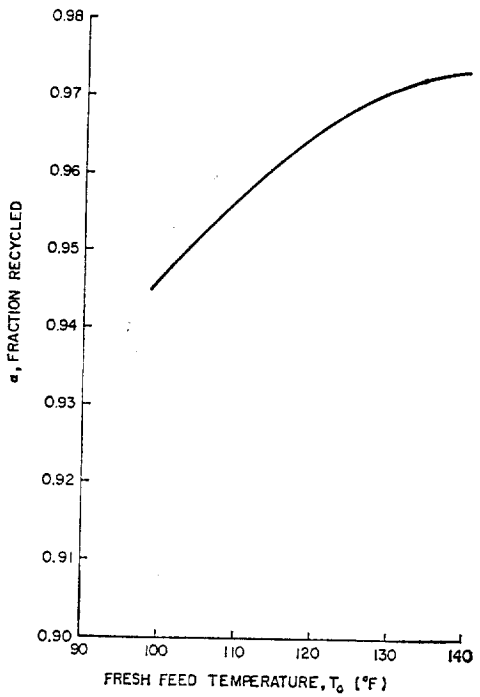

Fig. 6 Fresh feed temperature vs. recycle ratio at the following conditions: $T-T_1=4°F$, $W_1=400$ ft³./hr., $T=65°F$.

Figure 6 illustrates the relationship between the fraction of the product stream recycled and the fresh feed temperature. For each data point the total throughput rate(W_1) and product stream composition are identical. The result indicates that although the production rate remains the same, significantly more material must be recycled internally as the feed temperature increases. This is ccnsistent with the theory as is evidenced by examination of the equation for the total heat flow in terms of the temperature drop in the recycle stream:

$$Q=62.43\left[\frac{\alpha}{1-\alpha}\right]W_1(T-T)_1 \tag{43}$$

Thus, designing the cystallizer to operate at high feed temperature can result in both increased installation and operating cost due to the higher recirculation rate.

At this point it is necessary to distinguish between the two types of particle size distributions that can be employed to illustrate crystallizer output. As noted above, the particle size distribution of the crystallizer product stream is expressed in terms of $f(r,t)$, a number density function. A weight density function would be of more practical value when comparing the effect of changes in steady state operating conditions on particle size. Therefore, subsequent results are reported in terms of the steady state particle size weight distribution $\bar{f}_W(r)$. This is obtained by solving the steady state particle balance equa tion which is now only a function of r:

$$G(C,T)V\frac{d\bar{f}}{dr}=\bar{\varepsilon}VB(C,T)\ \sigma(r-r_0)-(1-\alpha)W\bar{f} \tag{44}$$

in which the overbar (−) denotes steady state. This equation can be modified by the following substitutions:

$$\bar{\varepsilon}=1-K\bar{\mu}_3 \tag{45}$$

$$W_1=(1-\alpha)W \tag{46}$$

which results in and ordinary differential equation in terms of $\bar{f}(r)$:

$$G(C,T)\ V\frac{d\bar{f}(r)}{dr}=(1-K\bar{\mu}_3)\ B(C,T)\ \sigma(r-r_0)$$
$$V-W_1\bar{f}(r) \tag{47}$$

Equation (47) can be further simplified by combining terms:

$$A=\frac{W_1}{G(C,T)V} \tag{48}$$

$$D=\frac{(1-K\mu_3)}{G(C,T)}B(C,T) \tag{49}$$

This results in the standard form for a non-homogeneous ordinary differential equation:

$$\frac{d\bar{f}(r)}{dr}+A\bar{f}(r)=D\delta(r-r_0) \tag{50}$$

The Laplace transform with respect to $\bar{f}(r)$ is now applied to equation (50) with results with

$$\bar{f}(r)=\frac{(1-K\mu_3)}{G(C,T)}B(C,T)\ \mathrm{EXP}\left[\frac{W_1r}{G(C,T)V}\right] \tag{51}$$

in which use is made of $r_0 \cong 0$.

$\bar{f}(r)$ in equation (51) is expressed as the number of particles of size between r and $r+dr$ per ft.^{3} of crystallizer volume. In order to obtain the weight distribution, the unit particle weight is required. This is represented by the following expression:

$$\frac{\text{WEIGHT}}{\text{PARTICLE}} = \rho K r^3 \tag{52}$$

Multiplication of equation (51) by equation (52) results in the steady state particle size weight distribtion function:

$$\bar{f}_W(r) = \frac{\rho K r^3 (1-K\bar{\mu}_3)}{G(C, T)} B(C, T) \text{EXP}\left[\frac{-W_1 r}{G(C, T) V}\right] \tag{53}$$

in which $\bar{f}_W(r)$ is the steady state weight density function.

It should be noted that the weight distribution curve exhibits a maximum at the following point:

$$r_{max} = \frac{3G(C, T)V}{W_1} \tag{54}$$

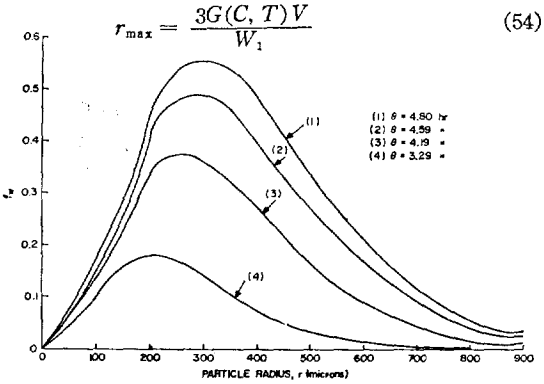

Fig. 7 Effect of residence time on particle size weight distribution at the conditions: $T_0 = 100°F$, $T = 65°F$, $C = 43.38$ lbm. ft^3., $C_0 = 43.48$ lbm. /ft^3.

Figures 7 through 9 illustrate the effect of residence time (V/W_1) on $\bar{f}_W$, on the particle size distribution moments, and on yield, respectively. In numerous industrial applications product particle size is of ultimate importance. Thus, in scaling up pilot plant data, residence time often proves to be the key parameter for designing the production unit ot deliver a product with acceptable screen specifications. The residence time is usually determined by setting the output rate and/or the crystallizer operating level via standard process control techniques (level and flow control).

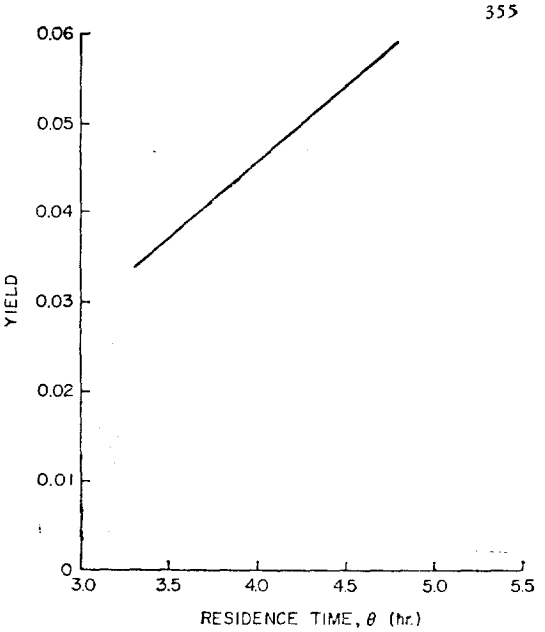

Fig. 8 Crystallizer yield vs. residence time at the the conditions: $T_0 = 100°F$, $T = 65°F$, $C = 43.38$ lbm. /ft^3., $C_0 = 43.48$ lbm. /ft^3.

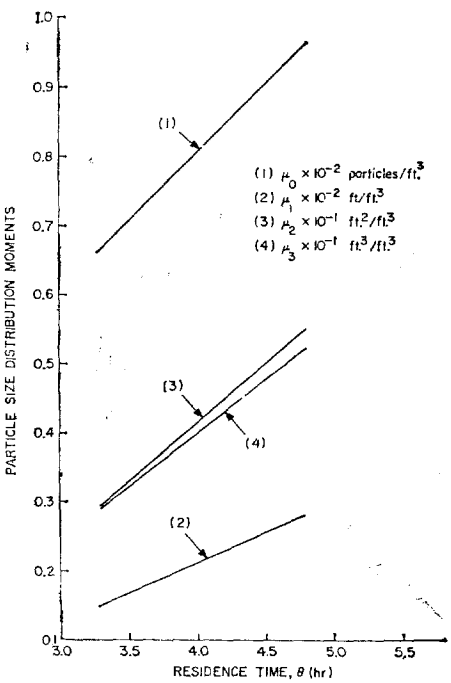

Fig. 9 Particle size distribution moments vs. residence time at the conditions: $T_0 = 100°F$, $T = 65°F$, $C = 43.38$lbm. /ft^3., $C_0 = 43.48$lbm. /ft^3.

As seen by the curves, the product stream particle size and yield can be increased by designing the unit to operate at higher residence times. However, in

most industrial units the amount of variation in operating level is relatively small due to equipment sizing. Thus, an **increase** in particle size is usually accompanied by a loss of production rate (via a decrease in W_1).

It should be noted that a linear dependence on residence time is exhibited by all output variables. In essence, the residence time controls the overall effect of the growth and nucleation rates.

5, 2 Application to On-Line Operating

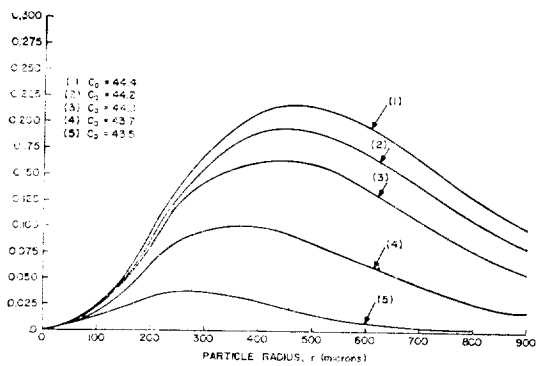

Fig. 10 Effect of fresh feed concentration on particle size weight distribution at the conditions: $T = 65°F$, $C = 43.4$lbm. /ft³., $W = 400$ ft.³/hr., $T = 130°F$.

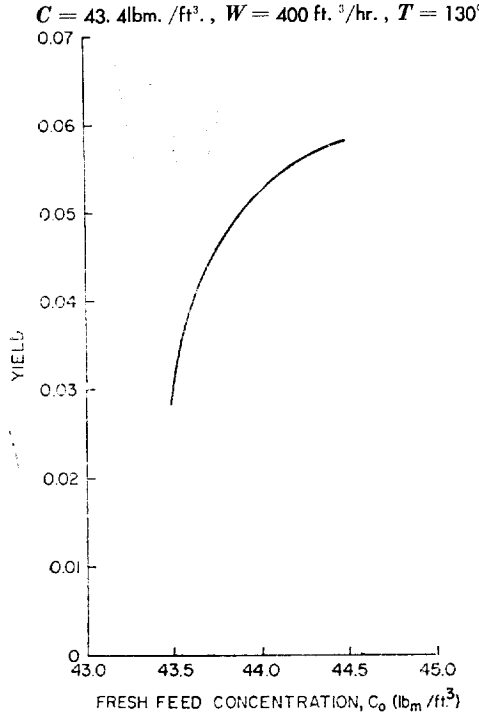

Fig. 11 Crystallizer yield vs. fresh feed concentration at the conditions: $T = 65°F$, $C = 43.4$ lbm. /ft³., $W = 400$ ft³. /hr. $T_0 = 130°F$.

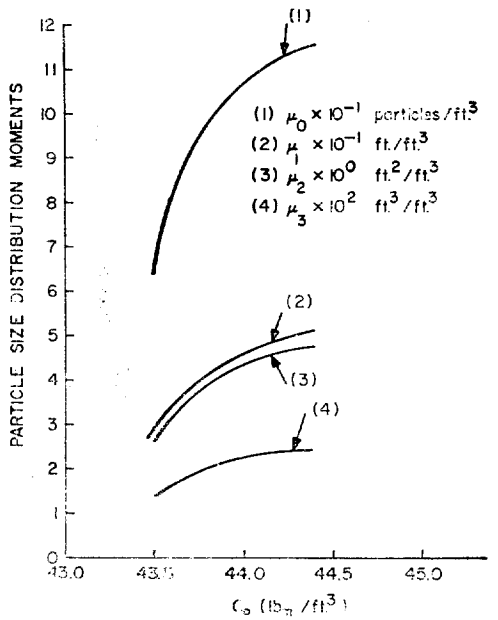

Fig. 12 Particle size distribution moments vs. fresh feed concentration at $T = 65°F$, $C = 53.4$ lbm. /ft³., $W = 400$ ft³. /hr., $T_0 = 130°F$.

Figures 10 through 12 illustrate the variation of crystallizer output (weight density distribution, yield, particle size distribution moments) due to changes in fresh feed concentration. In all cases the crystallizer operating temperature, concentration and fresh feed flow rate were maintained constant. Nonuniformity in fresh feed concentration is fresh-ly encountered in industry. As seen from the curves, particle size and yield vary directly with C_0. Thus, maintaining C_0 as high as possible ($C_0 > C$ where C is the crystallizer operating concentration) results in a coarser product and a higher yield. Obviously, a reduction in C_0 would be made in cases where reduced particle size is of ultimate importance. It should be emphasized that these relationships hold only for systems operating at a constant level of supersaturation

The solute concentration in the liquid fraction of the crystallizer magma determines the supersaturation at a given temperature Thus, the crystallizer output is strongly affected by fluctuations in operating concentration. Figures 13 and 14 illustrate the relationships between crystallizer output and concentration. In all caess the operating

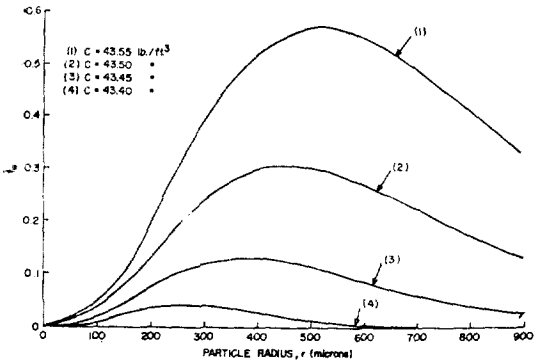

Fig. 13 Particle size weight distribution vs. operating concentration at $T = 65°F$, $T_0 = 130°F$, $W = 400 ft^3./hr.$, $C_0 - C = 1.0$ lbm./ft.^{3}

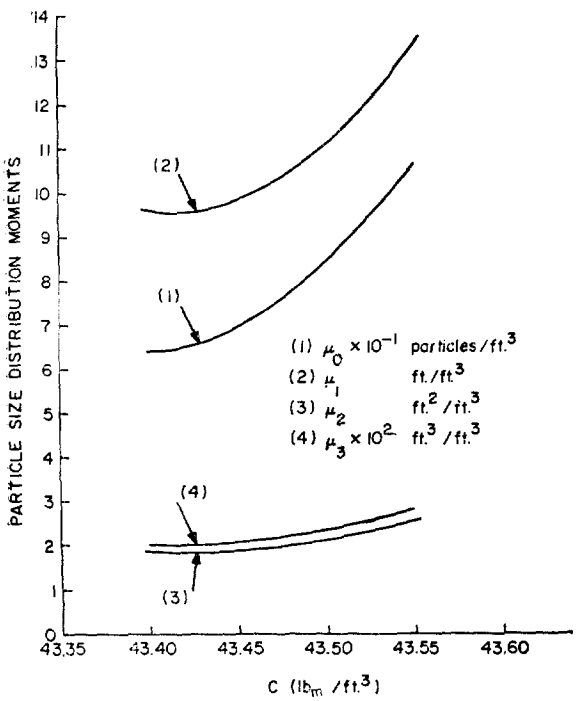

Fig. 14 Particle size distribution moments vs. operating concentration at $T=65°F$, $T_0=130°F$, $W=400$ ft^3./hr., $C_0-C=1.0$ lbm./ft^3.

temperature was held constant. In addition, (C_0-C) was held constant in order to maintain constant yield. As seen from the curves, raising C at **constant yield** and **temperature** results in increases in both the number and size of the particles. Thus, the crystallizer operate at a higher magma density and produces coarser grain.

The overall effect is more significant than that produced by manipulation of any of the other operating parameters previously investigated. This is due to the dependence of the growth and nucleation rates on supersaturation (variation of C at constant temperature results in changes in supersaturation). This is illustrated in Figure 14. The effect of operating concentration on the number of particles (μ_0) is more pronounced than that on particle size (μ_1, μ_2) due to the fact that B (nucleation rate) is a fourth order function of C whereas $G(C)$ is linear, as may be seen in Figure 15. Thus, the overall effect is directly related to the crystallization kinetics of the system. In this case the results of increasing C are magnified due to the fact that the yield was held constant by "raising" C_0. This may be easily understood from eq. (37).

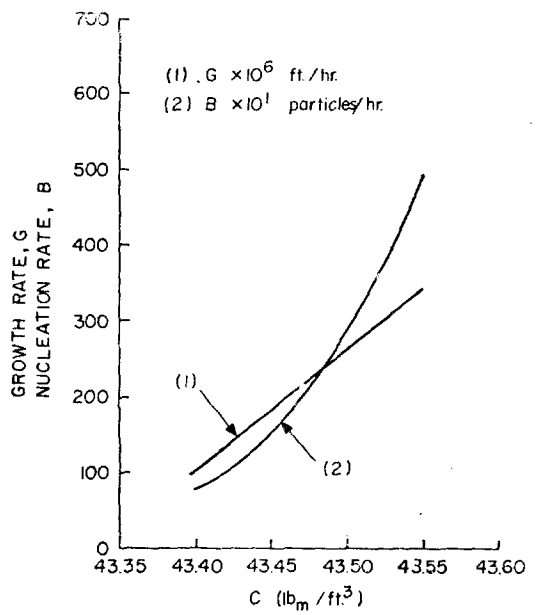

Fig. 15 Growth and nucleation rates vs. operating concentration at $T=65°F$, $C-C=1.0$ lbm./ft^3.

Under normal conditions where C_0 is invariant, an increase in C would produce a lower crystallization yield and a reduction in the total weight of particles per unit volume. However, the particle size weight distribution would still tend to be wider indicating an increase in particle size. In practice, on-line changes in operating concentration are extremely difficult to achieve. However, in the case of the unit used for this study a variation in supersaturation at constant temperature can be obtained by seeding the recycle stream.

Most industrial crystallizers, such as the type considered in this study, are designed to operate as a constant crystallization temperature. However, small fluctuations in temperature are known to occur over the operating cycle of the unit. Thus, by determining the magnitude of the effect of these variations on crystallizer output one can ascertain whether a temperature control system is required.

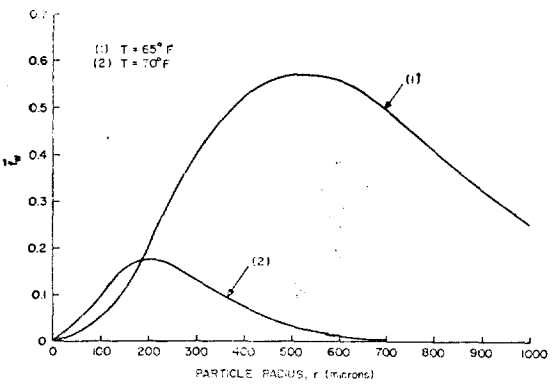

Fig. 16 Particle size weight distribution versus operating temperature at T_0=199°F, C_0=43.65 lbm./ft³., C=43.55 lbm./ft³., W=400 ft³./hr.

Figure 16 illustrates the effect of a 5°F increase in operating temperature on crystallizer output at constant C. It is seen that there is a significant reduction in particle size and yield. This effect is particular to the crystallization system, as may be revealed by examination of the grewth and nucleation rate expressions.

The situation is reversed if the temperature is increased at a **constant level of supersaturation,** as may be seen in Figure 17. In this case the data was obtained at constant yield in order to magnify the overall effect. Here the temperature dependent terms predominate and the increase in growth and nucleation rate result in a **coarser product** at a **higher** temperature. The magnitude of these effects indicates that for this system temperature control is mandatory so as to avoid wide fluctuations in product size and production rate.

6. Conclusions

The results of this study illustrate that the application of standard material and energy balance equations which completely describe the steady state operation of the unit. The system equations can be readily solved provided that the crystallization kinetics of the solute-solvent system are expressed as functions of temperature and concentration.

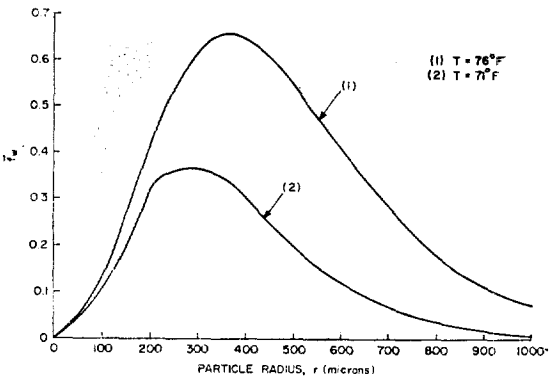

Fig. 17 Particle size weight distribution versus operating temperature at constant supersaturation and yield at T_0=100°F, C_0=46.12 lbm./ft³.

The application the of cooling-type crystallzer model in process design and atual plant operation was demonstrated through a complete analysis of a hypothetial crystallization system. This phase of the investigation resulted in the development of well defined functional relationships between process variables. The generation of process design curves from the model was accomplished without having to accumulate and evaluate a large array of experimental data. Significant results in this phase of the study include the variation of particle size distribution and yield with residence time and the effect of fresh feed temperature on recirculation rate.

The importance of controlling the fresh feed concentration and operating temperature was illustrated by determing the sensitivity of crystallizer output to changes in these variables. Since the model enables one to isolate and compare individual effects, it is possible to select a set of operating conditions that results in a desired yield (or (PSD). In some cases these relationships are not readily determined via the standard technique of "on line experimentation." A result of this type is the increase in product particle size obtained by operating the unit at higher tem-

peratures at constant supersaturation.

As indicated previously, the actual data produced by this study are specific to the crystallization system chosen to test the model and any conclusions drawn from these data cannot, in a rigorous sense, be further generalized. However, the techniques and methods of application can be easily extended to all types of industrial crystallizers (i. e. evaporation, vacuum cooling, vacuum evaporation). This form of steady state analysis of continuous crystallizers is a distinct improvement over present methods. However, the requirement of accurate expressions for the nucleation and growth rate proves to be the most difficult problem to overcome when applying this technique to other systems (as opposed to the development of the particle and energy balance equations). The extension of growth and nucleation rate expressions determined in a laboratory to plant scale is far from being free from error due to the contributing effects of agitation, vessel design and particle attrition. Thus, any inaccuracies in these expressions will be reflected in the data produced by the model.

Another direct application of the simulation model is the development of crystallizer control systems. The basic starting point of modern control theory is the linearization of unsteady state equations about a steady state control point. The simulation model can thesefore provide both the desired contsol variable and the point about which the controller is to operate. This can theoretically be accomplished without the necessity of having on-line operating data.

In summary, the development of this type of general approach to the steady state analysis of continuous crystallizers has provided a new dimension to the available technology of an important chemical engineering process.

Nomenclature

A_i inside heat transfer surface area, ft².
A_0 outside heat transfer surface area, ft².
B nucleation rate, particles/ft³.hr.
C crystallizer operating concentration, lbm./ft³.
C_0 fresh feed concentration, lbm. 1ft³.
C_s saturation concentration, lbm./ft³.
C_{pf} specific heat of fresh feed, Btu/lbm.°F
C_{pd} specific heat of product stream, Btu/lbm.°F
C_{pm} specific heat of crystallizer magma, Btu/lbm.°F
C_{pr} specific heat of recycle stream, Btu/lbm. °F.
D_i inside heat exchanger tube diameter, ft.
D_0 outside heat exchanges tube diameter, ft.
$f(r, t)$ particle size numbes distribution, number/ft³. /sec.
$\bar{f}(r)$ steady state particle size number distribution, number/ft³.
$\bar{f}_W(r)$ steady state particle size weight distribution, lbm./ft³.
G growth rate, ft./hr.
H_C heat of crystallization, Btu/lbm.
K shape factor for unit crystal.
n number of heat exchanger tubes.
Q total system heat flow, Btu/hr.
r particle size, ft.
r_0 size at which new crystals nucleate, ft.
r_{max} radius at which $\bar{f}_W$ has an absolute maximum.
S_1 percent supersaturation.
t time, sec.
T crystallizer operating temperature, °F.
T_0 fresh feed temperature, °F.
T_1 recycle stream temperature, °F.
ΔT_{lm} logarithmic mean temperature difference, °F.
U_0 overall heat transfer coefficient based on outside area, Btu/hr. ft².°F
V crystallizer operating volume, ft³.
W total crystallizer discharge flow rate, ft³./hr.
W_1 fresh feed flow rate, ft³./hr.
X mole fraction solute.
Y crystallizer yiteld.
α fraction of crystallizer output recycled.
ε volume fractiion of solution.
θ residence time, hr.
μ_0 zeroth moment of particle size number of crystals per unit volume, number/ft³.
μ_1 first moment of particle size, number distribution, total particle size per unit volume, ft./ft³.
μ_2 second moment of particle size number distribution total surface area per unit volume, ft²./ft³.
μ_3 third moment of particle size number distribution total volume per unit volume, ft³./ft³.

ν heat exchanger tubular velocity, ft./sec.
ν_{max} maximum heat exchanger tubular velocity, ft./sec.
ρ density of crystal, lbm./ft^3.
ρ_f density of fresh feed solution, lbm./ft^3.
ρ_d density of crystallizer discharge, lbm./ft^3.
ρ_m density of crystallizer magma, lbm./ft^3.
ρ_r density of recycle stream, lbm./ft^3.

References

1. H. M. Hulbert and S. Katz, *Chem. Engng. Sci.*, **19**, 555 (1964).
1. A. D. Randolph and M. A. Larson, *AIChE J.*, **8**, 639 (1962).
3. J. W. Mullin, Crystallization, Butterworths, London, England, 1961.
4. A. Van Hook, Crystallization: Theory and Practice, Reinhold Publishing Corp., NewYork, N. Y. 1961.
5. R. Sherwin, R. Shinnar and S. Katz, *AIChE J.*, **13**, 1141 (1967).
6. C. D. Han, *Chem. Engng. Sci.*, **22**, 611 (1967).
7. C. D. Han, *Ind. Engng. Chem. Process Design & Develop.*, **8**, 150(1969).
8. J. N. Robinson and J. E. Roberts, *Can. J. Chem. Engng.*, **35**, 105 (1957).
9. W. C. Saeman, *AIChE J.*, **1**, 107 (1956).
10. C. D. Han and R. Shinnar, *AIChE J.*, **14**, 612 (1968).
11. S. H. Bransom and D. E. Brown, paper presented at the symposium on Industrial Crystallization, London, England, April 1969.
12. R. C. Weast, Ed., Handbook of Chemistry and Physics, 44th Edition, p. 1699, The Chemical Rubber Co., 1961.
13. D. E. Garret and G. P. Rosebaum, *Chem. Engng.*, **65**, No. 11, 132(1958).
14. D. B. Wilson, *Chem. Engng.*, **72**, No. 12, 130 (1965).